

Reaction of an Early-Transition-Metal η^2 -Silaacyl Complex with Pyridine. Diastereoselectivity in the Formation of a (2-Pyridyl)silylmethoxy Ligand

John Arnold, Hee-Gweon Woo, and T. Don Tilley*

Chemistry Department, D-006, University of California at San Diego, La Jolla, California 92093

Arnold L. Rheingold* and Steven J. Geib

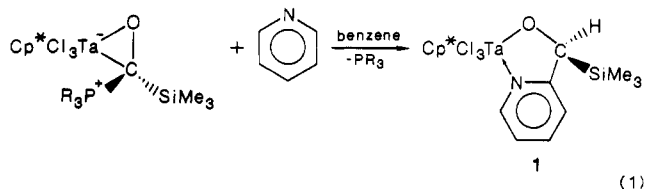
Department of Chemistry, University of Delaware, Newark, Delaware 19716

Received April 13, 1988

Zirconium and hafnium silyls $\text{Cp}^*\text{Cl}_2\text{MSi}(\text{SiMe}_3)_3$ ($\text{Cp}^* = \eta^5\text{-C}_5\text{Me}_5$; $\text{M} = \text{Zr}$, 2; $\text{M} = \text{Hf}$, 3) react with carbon monoxide to give unstable η^2 -silaacyl derivatives, $\text{Cp}^*\text{Cl}_2\text{M}[\eta^2\text{-COSi}(\text{SiMe}_3)_3]$ ($\text{M} = \text{Zr}$, 4; $\text{M} = \text{Hf}$, 5), which have been characterized by low-temperature NMR spectroscopy. The hafnium derivative 5 is trapped with pyridine to give one diastereomer of $\text{Cp}^*\text{Cl}_2\text{HfOC}(\text{H})[\text{Si}(\text{SiMe}_3)_3](o\text{-C}_5\text{H}_4\text{N})$ (6a) in high yield. Diastereomer 6a, formed in a highly diastereoselective process, has been characterized by elemental analysis, by IR and NMR spectroscopy, and by a single-crystal X-ray diffraction study. Crystals of 6a are orthorhombic, *Pccn*, with $a = 44.85$ (2) Å, $b = 9.401$ (3) Å, $c = 16.472$ (5) Å, $V = 6944$ (5) Å³, $Z = 8$, $R_F = 5.06\%$, and $R_{wF} = 5.56\%$. The crystal structure shows 6a to be the diastereomer with the Cp^* ligand and the $\text{Si}(\text{SiMe}_3)_3$ group on opposite sides of the HfOC_2N chelate ring. From reaction of $\text{Cp}^*\text{Cl}_2\text{Hf}(\text{C},\text{N}-\eta^2\text{-NC}_5\text{H}_4)$ with the formylsilane $(\text{Me}_3\text{Si})_3\text{SiCHO}$, compound 6a (40%) and its diastereomer 6b (60%) are obtained. This result is discussed with respect to the mechanism of the carbonylation reaction.

Introduction

Early-transition-metal η^2 -acyl complexes have been studied extensively and have provided a number of unusual reactivity modes for acyl functionalities.¹ Our investigations of η^2 -silaacyl complexes have afforded examples of remarkable electrophilic character for silaacyl carbonyl groups.² In some cases an η^2 -silaacyl ligand can bind Lewis bases to form stable complexes such as $\text{Cp}^*\text{Cl}_3\text{Ta}[\eta^2\text{-OC}(\text{L})(\text{SiMe}_3)]$ ($\text{Cp}^* = \eta^5\text{-C}_5\text{Me}_5$; $\text{L} = \text{py}$, PR_3).^{2c} In the course of studies on the latter compounds, we discovered that the phosphine adducts react with pyridine to form the pyridine-substituted tantalum complex 1 (eq 1).^{2h} It seemed that this reaction might proceed



(1) Leading references include: (a) Moloy, K. G.; Fagan, P. J.; Manriquez, J. M.; Marks, T. J. *J. Am. Chem. Soc.* 1986, 108, 56. (b) Wolczanski, P. T.; Bercaw, J. E. *Acc. Chem. Res.* 1980, 13, 121. (c) Martin, B. D.; Matchett, S. A.; Norton, J. R.; Anderson, O. P. *J. Am. Chem. Soc.* 1985, 107, 7952. (d) Tatsumi, K.; Nakamura, A.; Hofmann, P.; Stauffert, P.; Hoffmann, R. *J. Am. Chem. Soc.* 1985, 107, 4440. (e) Jeffery, J.; Lappert, M. F.; Luong-Thi, N. T.; Webb, M.; Atwood, J. L. *J. Chem. Soc., Dalton Trans.* 1981, 1593. (f) Gell, K. I.; Posin, G.; Schwartz, J.; Williams, G. M. *J. Am. Chem. Soc.* 1982, 104, 1846. (g) Erker, G. *Acc. Chem. Res.* 1984, 17, 103. (h) Fanwick, P. E.; Kobriger, L. M.; McMullen, A. K.; Rothwell, I. P. *J. Am. Chem. Soc.* 1986, 108, 8095. (i) Marsella, J. A.; Moloy, K. G.; Caulton, K. G. *J. Organomet. Chem.* 1980, 201, 389. (j) Fachinetti, G.; Fochi, G.; Floriani, C. *J. Chem. Soc., Dalton Trans.* 1977, 1946. (k) Young, S. J.; Hope, H.; Schore, N. E. *Organometallics* 1984, 3, 1585. (l) Klei, E.; Teuben, J. H. *J. Organomet. Chem.* 1981, 222, 79. (m) Moore, E. J.; Straus, D. A.; Armantrout, J.; Santarsiero, B. D.; Grubbs, R. H.; Bercaw, J. E. *J. Am. Chem. Soc.* 1983, 105, 2068.

(2) (a) Tilley, T. D. *J. Am. Chem. Soc.* 1985, 107, 4084. (b) Arnold, J.; Tilley, T. D. *J. Am. Chem. Soc.* 1985, 107, 6409. (c) Arnold, J.; Tilley, T. D.; Rheingold, A. L. *J. Am. Chem. Soc.* 1986, 108, 5355. (d) Campion, B. K.; Falk, J.; Tilley, T. D. *J. Am. Chem. Soc.* 1987, 109, 2049. (e) Arnold, J.; Tilley, T. D.; Rheingold, A. L.; Geib, S. J. *Inorg. Chem.* 1987, 26, 2556. (f) Arnold, J.; Tilley, T. D.; Rheingold, A. L.; Geib, S. J. *J. Chem. Soc., Chem. Commun.* 1987, 793. (g) Elsner, F. H.; Woo, H.-G.; Tilley, T. D. *J. Am. Chem. Soc.* 1988, 110, 313. (h) Arnold, J.; Tilley, T. D.; Rheingold, A. L.; Geib, S. J.; Arif, A. M. *J. Am. Chem. Soc.*, in press. (i) Roddick, D. M.; Heyn, R. H.; Tilley, T. D. *Organometallics*, in press. (j) Elsner, F. H.; Tilley, T. D.; Rheingold, A. L.; Geib, S. J. *J. Organomet. Chem.*, in press.

through a silaacyl complex with pyridine bound to tantalum, i.e. $\text{Cp}^*\text{Cl}_3\text{Ta}(\text{py})(\eta^2\text{-COSiMe}_3)$. However such an intermediate could not be observed, and reaction of pyridine with $\text{Cp}^*\text{Cl}_3\text{Ta}(\eta^2\text{-COSiMe}_3)$ gives only $\text{Cp}^*\text{Cl}_3\text{Ta}[\eta^2\text{-OC}(\text{py})(\text{SiMe}_3)]$. Here we report the generation of unstable η^2 -silaacyl derivatives of zirconium and hafnium and a trapping reaction of the hafnium derivative involving insertion of the silaacyl carbon into the ortho C-H bond of pyridine.

Results and Discussion

Preparations of zirconium and hafnium silyls $\text{Cp}^*\text{Cl}_2\text{MSi}(\text{SiMe}_3)_3$ (2, $\text{M} = \text{Zr}$; 3, $\text{M} = \text{Hf}$) from $(\text{THF})_3\text{LiSi}(\text{SiMe}_3)_3$ and Cp^*MCl_3 ^{4,5} are straightforward.⁶ Both 2 and 3 react rapidly (<5 min) under 1 atm of carbon monoxide at 22 °C in benzene-*d*₆ to give bright pink solutions that are characteristic for group 4 metal η^2 -silaacyl complexes.^{2a,d,g,i,j} These solutions are not stable at room temperature and turn colorless within 10 min. The ¹H NMR spectra of these colorless solutions are exceedingly complex, indicating decomposition to a number of products. Accordingly, several preparative-scale carbonylation reactions in various solvents (pentane, benzene, and diethyl ether) failed to yield isolable, pure products.

These carbonylation reactions were followed by variable-temperature ¹³C NMR using 91% ¹³C-enriched carbon monoxide in toluene-*d*₈. At -40 °C both 2 and 3 react with ¹³CO to give pink solutions that are stable for at least 1 h. Analysis of these solutions by ¹³C NMR spectroscopy revealed only the presence of an intense peak due to free ¹³CO at δ 183 and a resonance that can be assigned to an η^2 -silaacyl derivative^{2a-d,g-j}—at δ 405 for $\text{Cp}^*\text{Cl}_2\text{Zr}[\eta^2\text{-}^{13}\text{COSi}(\text{SiMe}_3)_3]$ (4) and at δ 389 for $\text{Cp}^*\text{Cl}_2\text{Hf}[\eta^2\text{-}^{13}\text{COSi}(\text{SiMe}_3)_3]$ (5). No other resonances attributable to ¹³C-enriched species were detected at this temperature. On warming above -10 °C, these low-field resonances at ca. 400 ppm diminish in intensity and completely disappear

(3) Gutekunst, G.; Brook, A. G. *J. Organomet. Chem.* 1982, 225, 1.

(4) Wolczanski, P. T.; Bercaw, J. E. *Organometallics* 1982, 1, 793.

(5) Blenkins, J.; DeLiefde Meijer, H. J.; Teuben, J. H. *J. Organomet. Chem.* 1981, 218, 383.

(6) Arnold, J.; Roddick, D. M.; Tilley, T. D.; Rheingold, A. L.; Geib, S. J. *Inorg. Chem.*, in press.

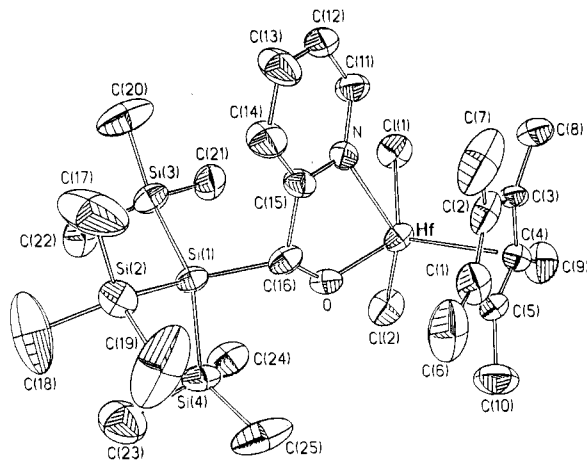
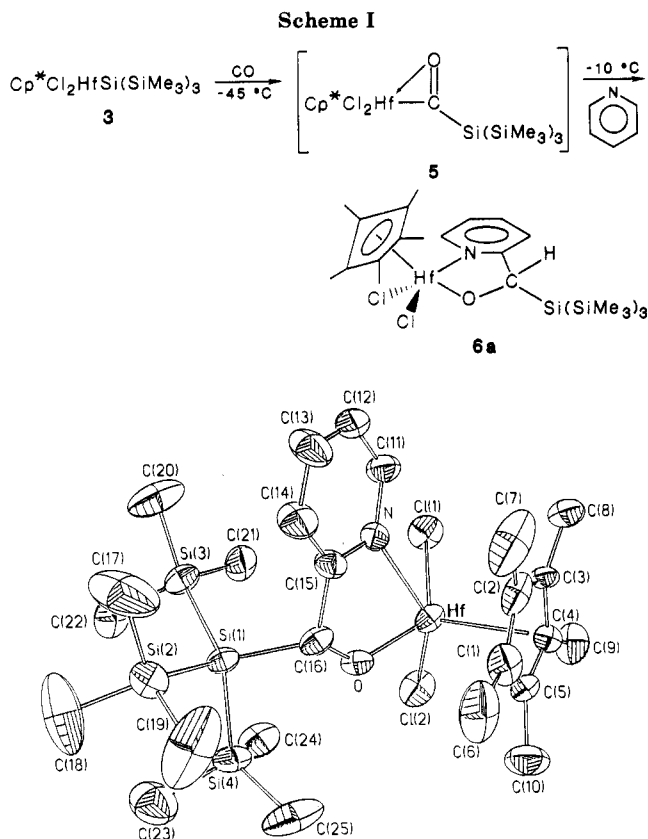


Figure 1. ORTEP view of **6a** with atom-labeling scheme. Thermal ellipsoids are at 50% probability.

by the time the NMR probe is warmed to 20 °C.

In order to further characterize these transient η^2 -silaacyl complexes, we attempted to form more stable Lewis base adducts of the type $\text{Cp}^*\text{Cl}_2\text{M}[\eta^2\text{-OC(L)Si(SiMe}_3)_3]$. It had previously been observed that the thermally sensitive silaacyl $\text{Cp}^*\text{Cl}_3\text{Ta}(\eta^2\text{-COSiMe}_3)$ forms stable, isolable phosphine adducts $\text{Cp}^*\text{Cl}_3\text{Ta}[\eta^2\text{-OC(PR}_3)_2\text{(SiMe}_3)]$.^{2c,e,h} In contrast, similar adducts of **4** and **5** were not observed. Carbonylations (ca. 1 atm) of **2** or **3** in the presence of PMe_3 or PCy_3 at 22 °C in benzene- d_6 yielded complex mixtures of products (by ^1H NMR). As judged by ^1H NMR, these carbonylation reactions were not influenced by the presence of the phosphines.

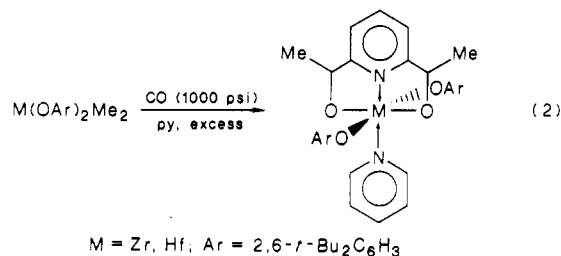
Reaction of **2** and carbon monoxide (1 atm) in the presence of pyridine (2 equiv) was similarly unsuccessful. However, carbonylation of hafnium silyl **3** in the presence of pyridine (2 equiv) resulted in smooth conversion to the colorless, crystalline product **6a** in high yield (Scheme I). Characterization of **6a** is based on elemental analysis, on infrared and NMR spectroscopy, and on a single-crystal X-ray diffraction study (Figure 1). Note that at -10 °C or room temperature this reaction produces only the diastereomer indicated ($\geq 99\%$ by ^1H NMR), with the Cp^* and $\text{Si(SiMe}_3)_3$ groups as trans substituents in the HfOC_2N ring.

The reaction in Scheme I was followed by variable-temperature ^{13}C NMR spectroscopy using labeled ^{13}CO in toluene- d_8 solvent. The η^2 -silaacyl **5**- ^{13}C formed at -45 °C in the absence of pyridine. Addition of pyridine (2 equiv) at this temperature caused no change in the spectrum. This contrasts with the situations found for the related tantalum η^2 -silaacyl $\text{Cp}^*\text{Cl}_3\text{Ta}(\eta^2\text{-COSiMe}_3)$, which forms the silaacyl adduct $\text{Cp}^*\text{Cl}_3\text{Ta}[\eta^2\text{-OC(py)(SiMe}_3)]$ under these conditions, and for the η^2 -acyl $\text{Cp}^*\text{Cl}_3\text{Ta}(\eta^2\text{-COCH}_2\text{CMe}_3)$, which forms the metal-bound pyridine adduct $\text{Cp}^*\text{Cl}_3\text{Ta(py)}(\eta^2\text{-COCH}_2\text{CMe}_3)$.^{2h} As the tem-

perature was raised to ca. -10 °C, a new ^{13}C NMR signal corresponding to complex **6a**- ^{13}C was observed. During the conversion of **5**- ^{13}C to **6a**- ^{13}C , no intermediate species were detected. These results seem to be most consistent with a mechanism involving pyridine coordination to hafnium, giving $\text{Cp}^*\text{Cl}_2\text{Hf(py)}[\eta^2\text{-COSi(SiMe}_3)_3]$, which rapidly rearranges to **6a** (see Scheme II).

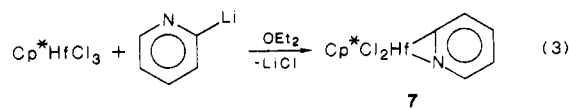
If the reaction in Scheme I takes place in a 1:1 mixture of pyridine and pyridine- d_5 , 50% incorporation of deuterium into the $\text{OCH}[\text{Si(SiMe}_3)_3]$ position of **6a** is observed (by ^1H NMR). This indicates that the step involving C-H bond breaking follows the rate-determining step of the reaction. The same result was obtained for the reactions shown in eq 2^{1h} and 2.^{1h}

Recently, reaction of the dialkyls $\text{M(OAr)}_2\text{Me}_2$ ($\text{M} = \text{Zr, Hf}$; $\text{OAr} = 2,6\text{-}t\text{-Bu}_2\text{C}_6\text{H}_3$) with carbon monoxide and pyridine was reported to give similar products resulting from insertion of acyl ligands into both ortho C-H bonds of pyridine (eq 2).^{1h} In this reaction, both meso and threo



diastereomers in a 1:1 ratio were observed. It was suggested that this process occurs by nucleophilic attack of an η^2 -acyl onto a coordinated pyridine ring (analogous to path a, Scheme II). A second possible mechanism involves abstraction of a pyridine hydrogen by the η^2 -acyl ligand to afford an orthometalated ($\text{C,N-}\eta^2$)-pyridine complex (path b, Scheme II). Similar abstraction processes have been observed in titanium,⁷ scandium,⁸ tantalum,⁹ zirconium,¹⁰ and yttrium¹¹ systems.

To test the feasibility of path b in Scheme II, the ($\text{C,N-}\eta^2$)-pyridine complex $\text{Cp}^*\text{Cl}_2\text{Hf}(\text{C,N-}\eta^2\text{-C}_5\text{H}_4\text{N})$ (**7**) was prepared by reaction of Cp^*HfCl_3 with 2-lithiopyridine in diethyl ether (eq 3). Biege **7** was isolated in 79% yield



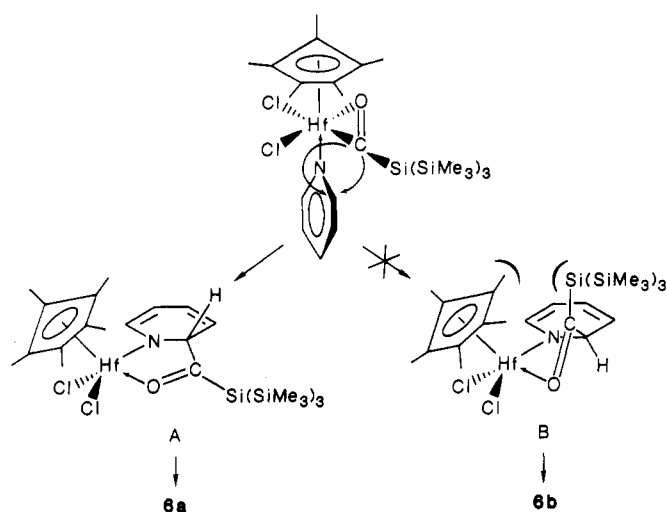
(7) Klei, B.; Teuben, J. H. *J. Chem. Soc., Chem. Commun.* **1978**, 659.
 (8) Thompson, M. E.; Baxter, S. M.; Bulls, A. R.; Burger, B. J.; Nolan, M. C.; Santarsiero, B. D.; Schaefer, W. P.; Bercau, J. E. *J. Am. Chem. Soc.* **1987**, *109*, 203.

(9) McLain, S. J.; Schrock, R. R.; Sharp, P. R.; Churchill, M. R.; Youngs, W. J. *J. Am. Chem. Soc.* **1979**, *101*, 263.

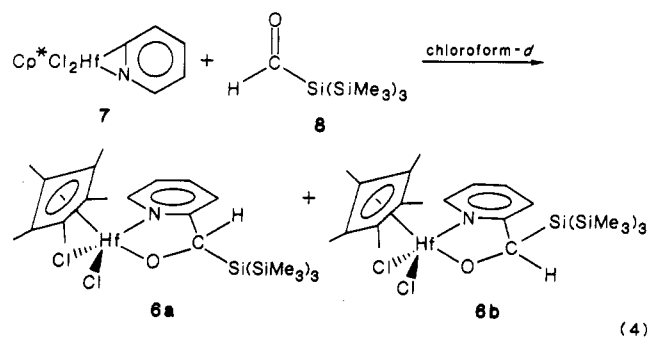
(10) Buchwald, S. L.; Watson, B. T.; Huffman, J. C. *J. Am. Chem. Soc.* **1986**, *108*, 7411.

(11) den Haan, K. H.; Wielstra, Y.; Teuben, J. H. *Organometallics* **1987**, *6*, 2053.

Scheme III



by vacuum sublimation. Its characterization is based on elemental analysis and infrared and NMR spectroscopy. Properties of **7** are similar to those reported for the analogous compounds $\text{Cp}^*\text{Sc}(\text{C}(\text{C},\text{N}-\eta^2-\text{C}_5\text{H}_4\text{N}))^8$ and $\text{Cp}^*\text{Y}(\text{C}(\text{C},\text{N}-\eta^2-\text{C}_5\text{H}_4\text{N}))^{11}$. As shown in eq 4, **7** reacts rapidly



with the formylsilane $(\text{Me}_3\text{Si})_3\text{SiCHO}$ (**8**)^{2g} to give two products, **6a** (40%) and its diastereomer **6b** (60%), as shown by ¹H NMR. This result demonstrates that reaction involving an insertion such as that depicted in path b is possible. However, the fact that both diastereomers are formed in the above reaction but not in the reaction of Scheme I rules out *free* formylsilane as an intermediate in the carbonylation.

The diastereoselectivity observed in the carbonylation reaction can be explained by the mechanism represented by path a, Scheme II. In the pyridine complex $\text{Cp}^*\text{Cl}_2\text{Hf}(\text{py})[\eta^2-\text{COSi}(\text{SiMe}_3)_3]$, attack of the silaacyl carbon onto the pyridine ring can theoretically occur in two ways (Scheme III), resulting in two different geometries (A and B) that will control the stereochemistry of the products. Suprafacial 1,2 hydrogen shifts would then transform A into diastereomer **6a** and B into diastereomer **6b**. Greater steric interactions between the Cp^* and $\text{Si}(\text{SiMe}_3)_3$ groups in B should lead to a higher energy intermediate (or transition state); therefore, the reaction pathway leading to **6b** is less favored.

Description of the Structure of 6a. The molecular structure and atom-labeling scheme are shown in Figure 1. Relevant geometrical parameters are summarized in Tables II and III. The molecule adopts a pseudo-square-pyramidal coordination geometry, with the Cl(1), Cl(2), O, and N atoms at the basal positions. The N, C(15), C(16), and O atoms of the chelate ring are planar within experimental error, and Hf lies 0.3881 (5) Å out of this plane. The least-squares plane formed by N, C(15), C(16), and O is tilted 2.9° from the plane defined by the chelate

Table I. Crystal, Data Collection, and Refinement Parameters

(a) Crystal Parameters			
formula	$\text{C}_{25}\text{H}_{47}\text{NOSi}_4\text{Cl}_2\text{Hf}$	$V, \text{Å}^3$	6945 (5)
cryst syst	orthorhombic	Z	8
space group	$Pccn$	$D(\text{calcd}), \text{g cm}^{-3}$	1.41
$a, \text{Å}$	44.85 (2)	temp, °C	23
$b, \text{Å}$	9.401 (2)	μ, cm^{-1}	34.7
$c, \text{Å}$	16.472 (5)	cryst dims, mm	0.13 × 0.40 × 0.40
(b) Data Collection			
diffractometer	Nicolet R3m/μ	scan speed, deg/min	variable, 6–20
radiation	Mo $K\alpha$ ($\lambda = 0.71073 \text{ Å}$)	reflections	5799
scan technique	ω	collected unique data	5139
2θ scan range, deg	$4^\circ \leq 2\theta \leq 47^\circ$	unique data, $F_o \geq 5\sigma(F_o)$	2969
data collected	$+h, +k, +l$		
(c) Refinement			
$R_F, \%$	5.06	GOF	1.020
$R_{wF}, \%$	5.56	data/parameter	9.64
mean shift/esd max	0.09	g^a	0.0013
$^a w^{-1} = \sigma^2(F_o) + gF_o^2.$			

Table II. Atomic Coordinates ($\times 10^4$) and Isotropic Thermal Parameters ($\text{Å}^2 \times 10^3$)

	x	y	z	U^a
Hf	721.1 (1)	5367.1 (6)	6690.9 (3)	49.1 (2)
Cl(1)	485 (1)	3118 (4)	6314 (3)	77 (2)
Cl(2)	867 (1)	5678 (4)	5281 (2)	83 (2)
Si(1)	1670 (1)	4642 (4)	7576 (2)	49 (1)
Si(2)	1994 (1)	5201 (5)	8661 (3)	68 (2)
Si(3)	1653 (1)	2186 (4)	7313 (3)	64 (2)
Si(4)	1836 (1)	5827 (4)	6402 (3)	71 (2)
O	1136 (2)	5733 (9)	7025 (5)	55 (3)
N	817 (2)	4062 (11)	7886 (6)	51 (4)
C(1)	596 (3)	7655 (18)	7371 (11)	81 (6)
C(2)	406 (3)	6644 (15)	7712 (8)	70 (6)
C(3)	200 (3)	6161 (12)	7101 (9)	57 (5)
C(4)	280 (3)	6931 (13)	6387 (8)	52 (5)
C(5)	512 (3)	7792 (14)	6552 (8)	63 (5)
C(6)	833 (4)	8562 (20)	7789 (13)	131 (10)
C(7)	385 (5)	6316 (23)	8602 (10)	159 (13)
C(8)	-48 (4)	5151 (17)	7200 (13)	177 (10)
C(9)	119 (4)	6772 (18)	5581 (8)	92 (7)
C(10)	644 (4)	8898 (19)	5988 (12)	108 (9)
C(11)	647 (3)	3105 (15)	8277 (9)	70 (6)
C(12)	714 (4)	2610 (20)	9039 (10)	92 (7)
C(13)	950 (4)	3064 (23)	9406 (11)	106 (9)
C(14)	1137 (4)	4003 (20)	9039 (8)	84 (7)
C(15)	1071 (3)	4472 (14)	8249 (7)	53 (5)
C(16)	1275 (3)	5457 (14)	7786 (7)	53 (5)
C(17)	1919 (5)	4238 (30)	9644 (12)	211 (17)
C(18)	2382 (4)	4739 (28)	8419 (12)	179 (14)
C(19)	1967 (6)	7094 (20)	8884 (14)	203 (15)
C(20)	1595 (6)	1080 (20)	8235 (11)	143 (12)
C(21)	1353 (3)	1772 (15)	6557 (10)	88 (7)
C(22)	2018 (4)	1720 (16)	6874 (10)	96 (8)
C(23)	2248 (4)	5749 (23)	6292 (13)	139 (11)
C(24)	1674 (4)	5035 (17)	5464 (8)	91 (8)
C(25)	1718 (5)	7706 (19)	6458 (11)	150 (12)

^a Equivalent isotropic U defined as one-third of the trace of the orthogonalized U_{ij} tensor.

ring. Figure 2 provides a better view of the coordination geometry about Hf and the conformation of the fused rings. The Hf–C(Cp^*) and Hf–Cl bond lengths in the molecule are consistent with corresponding distances found in the related compounds $\text{Cp}^*\text{Cl}_2\text{HfSi}(\text{SiMe}_3)_3$,⁶ $\text{Cp}^*\text{Cl}_2\text{HfGe}(\text{SiMe}_3)_3$,⁶ $\text{Cp}^*\text{Hf}(2,3\text{-dimethyl-1,3-butadiene})\text{Cl}$,¹² $\text{Cp}^*\text{Hf}(2,3\text{-dimethyl-1,3-butadiene})\text{Cl}(\text{py})$,¹² and

Table III. Selected Bond Lengths and Angles^a

(a) Bond Lengths (Å)			
Hf-Cl(1)	2.445 (4)	C(15)-C(16)	1.51 (2)
Hf-Cl(2)	2.430 (4)	N-C(15)	1.34 (2)
Hf-O	1.969 (9)	C(16)-Si(1)	1.96 (1)
Hf-N	2.36 (1)	Hf-Cp*(CNT)	2.20 (1)
C(16)-O	1.42 (1)	Si(1)-Si(2)	2.362 (6)
C(16)-Si(1)	1.96 (1)	Si(1)-Si(3)	2.351 (5)
		Si(1)-Si(4)	2.353 (6)
(b) Bond Angles (deg)			
N-Hf-O	71.7 (3)	O-Hf-Cl(2)	89.6 (3)
N-Hf-Cl(1)	80.9 (3)	Cp*(CNT)-Hf-Cl(1)	113.3 (3)
N-Hf-Cl(2)	144.2 (3)	Cp*(CNT)-Hf-Cl(2)	109.2 (3)
Cp*(CNT)-Hf-N	106.4 (4)	Cl(1)-Hf-Cl(2)	88.7 (1)
Cp*(CNT)-Hf-O	115.1 (4)	N-C(15)-C(16)	117.8 (11)
O-Hf-Cl(1)	129.1 (3)	Hf-O-C(16)	129.0 (8)

^aCp*(CNT) is the centroid of the C₅Me₅ ring.

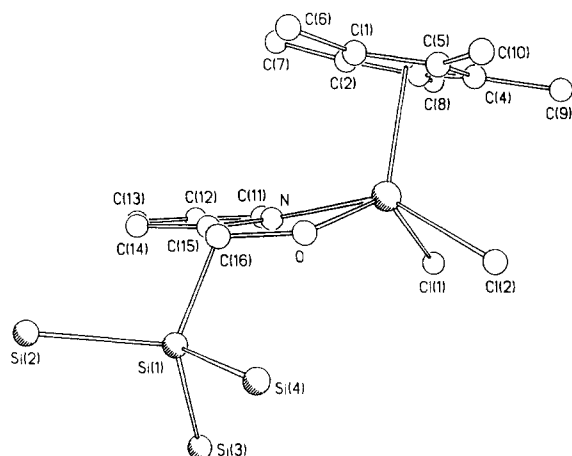


Figure 2. A different view of **6a**. Methyl groups on Si(2), Si(3), and Si(4) are omitted for clarity.

Cp*Cl₂Hf[η²-COP(CMe₃)₂].¹³

Experimental Section

Manipulations were performed under an inert atmosphere of nitrogen or argon by using standard Schlenk techniques or a Vacuum Atmospheres glovebox. Dry, oxygen-free solvents were employed throughout. Elemental analyses were performed by Schwartzkopf microanalytical laboratories. Infrared spectra were recorded on a Perkin-Elmer 1330 spectrometer. ¹H NMR spectra were recorded at 300 MHz with a GE QE-300 spectrometer or at 90 MHz with a Varian EM-390 instrument. ¹³C and ²⁹Si{¹H} NMR spectra were recorded at 75.5 and 59.6 MHz, respectively, on the GE QE-300. The zirconium and hafnium silyls Cp*Cl₂MSi(SiMe₃)₃ were prepared according to a procedure described elsewhere.⁸ Carbon monoxide (Liquid Carbonics) and 91% ¹³C carbon monoxide (MSD) were used as received. 2-Bromopyridine was distilled before use. The compounds Cp*HfCl₃⁵ and (Me₃Si)₃SiCHO²⁶ were prepared by literature methods.

Cp*Cl₂HfOC(H)[Si(SiMe₃)₃](*o*-C₅H₄N) (6a**).** A solution of Cp*Cl₂HfSi(SiMe₃)₃ (**5**) (0.30 g, 0.47 mmol) and pyridine (75 μL, 0.95 mmol) in benzene (10 mL) was pressurized with carbon monoxide (100 psi). After stirring for 4 h, the purple solution was evaporated and extracted with diethyl ether (30 mL). Following concentration (to ca. 10 mL) and cooling to -45 °C overnight, the product was isolated as small pale purple crystals in 74% yield (0.26 g). Recrystallization from cold diethyl ether gave colorless crystals (mp 255–258 °C dec) suitable for X-ray crystallography. Anal. Calcd for C₂₅H₄₇Cl₂HfNOSi₄: C, 40.6; H, 6.41; Cl, 9.59. Found: C, 40.6; H, 6.49; Cl, 9.88. IR (Nujol mull, CsI, cm⁻¹): 2720 w, 1601 m, 1264 sh, 1241 s, 1210 w, 1152 w, 1125 w, 1098 w, 1055 s, 1046 s, 1000 w, 973 m, 950 br, 830 s, 688 m,

642 w, 623 m, 557 m, 486 w, 346 m, 300 m, 278 m. ¹H NMR (chloroform-*d*, 300 MHz, 22 °C): δ 0.15 (s, 27 H, SiMe₃), 1.91 (s, 15 H, C₅Me₅), 6.26 (s, 1 H, OCH), 7.28 (t, *J* = 7 Hz, 1 H, py), 7.35 (d, *J* = 7 Hz, 1 H, py), 7.79 (t, *J* = 7 Hz, 1 H, py), 8.77 (d, *J* = 7 Hz, 1 H, py). ¹³C NMR (chloroform-*d*, 75.5 MHz, 22 °C): δ 1.73 (q, ¹J_{CH} = 120 Hz, SiMe₃), 11.36 (q, ¹J_{CH} = 127 Hz, C₅Me₅), 80.01 (d, ¹J_{CH} = 139 Hz, OCH), 120.5 (dd, *J* = 6, 163 Hz, py), 121.0 (dt, *J* = 6, 167 Hz, py), 122.3 (s, C₅Me₅), 138.4 (dd, *J* = 7, 165 Hz, py), 149.8 (dt, *J* = 5, 182 Hz, py), 174.8 (s, py). ²⁹Si{¹H} NMR (chloroform-*d*, 59.6 MHz, 22 °C): δ -65.15 (Si(SiMe₃)₃), -12.51 (Si(SiMe₃)₃).

Reaction of **5 with CO in Pyridine/Pyridine-*d*₅.** A pressure bottle was charged with Cp*Cl₂HfSi(SiMe₃)₃ (**5**) (0.40 g, 0.63 mmol), pyridine (0.051 mL, 0.63 mmol), pyridine-*d*₅ (0.050 mL, 0.63 mmol), and benzene (20 mL). The solution was pressurized with carbon monoxide (100 psi), after which it gradually turned to purple over ca. 20 min. After the solution was stirred for 4 h, the pressure was reduced and the volatile components were removed by evacuation. Extraction with diethyl ether (30 mL), concentration, and cooling to -40 °C gave purple crystals in 74% yield. Recrystallization from diethyl ether afforded colorless crystals. In the ¹H NMR spectrum of this sample, the ratio of integrated intensities for the C₅Me₅ and OCH protons of **6a** was 30:1.

Cp*Cl₂Hf(C,N-η²-C₅H₄N) (7**).** A solution of 2-bromopyridine (0.15 g, 0.95 mmol) in 20 mL of diethyl ether was added slowly to *n*-butyllithium (0.6 mL of a 1.6 M hexane solution, 0.96 mmol) at -78 °C, and the resulting red solution was stirred for 10 min. This cold solution of 2-lithiopyridine was then added to a suspension of Cp*HfCl₃ (0.40 g, 0.95 mmol) in diethyl ether and also at -78 °C. The reaction mixture was allowed to slowly warm to room temperature with stirring. After 1 day, the solution was evaporated to dryness and the resulting residue washed with 10 mL of pentane and dried in vacuo. Sublimation at 110–120 °C (10⁻² mmHg) afforded 0.35 g (80%) of **7** as a beige solid (mp 185–187 °C). Anal. Calcd for C₁₅H₁₉Cl₂HfN: C, 38.9; H, 4.14; N, 3.03. Found: C, 38.6; H, 4.38; N, 2.80. IR (Nujol, cm⁻¹): 2720 w, 1580 m, 1534 w, 1425 m, 1258 m, 1243 m, 1043 w, 1025 w, 1008 m, 772 s, 675 w, 635 w, 425 br, 390 w, 318 s, 303 s. ¹H NMR (benzene-*d*₆, 300 MHz, 22 °C): δ 1.87 (s, 15 H, C₅Me₅), 6.37 (t, *J* = 5.4 Hz, 1 H, py), 6.86 (t, *J* = 7.5 Hz, 1 H, py), 7.55 (d, *J* = 7.5 Hz, 1 H, py), 7.92 (d, *J* = 5.4 Hz, 1 H, py).

Reaction of **7 with (Me₃Si)₃SiCHO.** To Cp*Cl₂Hf(C,N-η²-C₅H₄N) (**7**, 0.02 g, 0.043 mmol) in 0.3 mL of chloroform-*d* was added (Me₃Si)₃SiCHO (0.045 mmol) dissolved in chloroform-*d* (0.02 mL). After 20 min, the ¹H NMR spectrum of the solution showed complete conversion to the diastereomers **6a** (40%) and **6b** (60%). For **6b**: ¹H NMR (chloroform-*d*, 300 MHz, 22 °C): δ 0.19 (s, 27 H, SiMe₃), 1.93 (s, 15 H, C₅Me₅), 7.04 (s, 1 H, OCHSi), 7.32 (m, 2 H, py), 7.68 (t, *J* = 7 Hz, 1 H, py), 8.31 (t, *J* = 7 Hz, 1 H, py).

Collection of Diffraction Data. Crystal data and the parameters used during the collection of diffraction data are contained in Table I. A colorless crystal of **6a** was sealed under nitrogen in a glass capillary. **6a** crystallizes in the orthorhombic space group *Pccn*. Unit cell dimensions were derived from the least-squares fit of the angular settings of 25 reflections with 20° ≤ 2θ ≤ 25°. Data were corrected for absorption by using the program XABS (H. Hope) which is based on deviations between *F*_o and *F*_c values. A profile fitting procedure was applied to all intensity data to improve the precision of the measurement of weak reflections. No significant decomposition occurred in three standard reflections during the course of data collection.

Solution and Refinement of Structure. The Hf atom was located via heavy-atom methods. Remaining non-hydrogen atoms were located from subsequent difference Fourier syntheses and were refined anisotropically. Hydrogen atom positions were calculated (*d*(C-H) = 0.96 Å, thermal parameters 1.2 times the isotropic equivalent for the carbon atom to which it was attached). The final difference Fourier synthesis showed only a diffuse background (0.74 e/Å³, near Hf). An inspection of *F*_o vs *F*_c values and trends based on sin θ, parity group, or Miller index failed to reveal any systematic error in the data. All computer programs used in the data collection and refinement are contained in the SHELXTL (5.1) program library (G. Sheldrick, Nicolet XRD, Madison, WI). Atomic coordinates are given in Table II, and

(13) Roddick, D. M.; Santarsiero, B. D.; Bercaw, J. E. *J. Am. Chem. Soc.* **1985**, *107*, 4670.

selected bond distances and angles in Table III.

Acknowledgment is made to the Air Force Office of Scientific Research, Air Force Systems Command, USAF, for support of this work under Grant AFOSR-85-0228. The U.S. Government is authorized to reproduce and distribute reprints for Governmental purposes notwithstanding any copyright notation thereon. T.D.T. thanks

the Alfred P. Sloan Foundation for a research fellowship (1988-1990).

Supplementary Material Available: Tables of bond distances and angles, anisotropic thermal parameters, and hydrogen atom coordinates for **6a** (4 pages); a listing of observed and calculated structure factors for **6a** (20 pages). Ordering information is given on any current masthead page.

Structure and Bonding in Transition-Metal Carbonyls and Nitrosyls. 3. Molecular Structure of Osmium Pentacarbonyl from Gas-Phase Electron Diffraction

Jinfan Huang,^{1a} Kenneth Hedberg,*^{1a} and Roland K. Pomeroy^{1b}

Departments of Chemistry, Oregon State University, Corvallis, Oregon 97331, and Simon Fraser University, Burnaby, British Columbia, Canada V5A 1S6

Received April 15, 1988

The molecular structure of osmium pentacarbonyl has been investigated by gas-phase electron diffraction. Corrections for three-atom multiple scattering were included. The data are consistent with a molecule of D_{3h} symmetry. Although the relative lengths of the axial and equatorial Os-C bonds could not be determined because of high correlations with several other parameters, the weight of the evidence strongly suggests that the axial bonds are the longer. Values for the bond lengths (r_g and r_{ax} ; r_{ax} should be comparable to distances determined by X-ray diffraction) and some of the principal vibrational amplitudes (l) with estimated 2σ uncertainties are $\langle r_g(\text{Os}-\text{C}) \rangle = 1.962$ (4) Å, $\langle r_{ax}(\text{Os}-\text{C}) \rangle = 1.955$ (4) Å, $\Delta r_g(\text{Os}-\text{C}) = r_g(\text{Os}-\text{C}_{ax}) - r_g(\text{Os}-\text{C}_{eq}) = 0.047$ (46) Å, $\Delta r_{ax}(\text{Os}-\text{C}) = 0.043$ Å, $\langle r_g(\text{C}=\text{O}) \rangle = 1.142$ (4) Å, $\langle r_{ax}(\text{C}=\text{O}) \rangle = 1.130$ (4) Å, $\Delta r_g(\text{C}=\text{O}) = \langle r_{ax}(\text{C}=\text{O}) \rangle - \langle r_g(\text{C}=\text{O}) \rangle = 0$ (assumed), $l(\text{Os}-\text{C}_{ax}) = l(\text{Os}-\text{C}_{eq}) - 0.003$ Å (assumed) = 0.046 (9) Å, $l(\text{C}=\text{O}_{ax}) = l(\text{C}=\text{O}_{eq})$ (assumed) = 0.043 (4) Å. The multiple scattering from $\text{Os}(\text{CO})_5$ was found to be small, and although the quality of the fit was improved by inclusion of multiple scattering corrections, the parameter values obtained with and without them were not significantly different.

Introduction

Two types of structure dominate the shapes of inorganic five-coordinate molecules in the gas phase, the tetragonal pyramid and the trigonal bipyramid with respective symmetries C_{4v} and D_{3h} . As expected from the well-known valence-shell electron-pair repulsion (VSEPR) theory,² the halogen pentafluorides, such as BrF_5 and IF_5 ,³ are of the first type and the pentahalides of atoms from group 15 and 5, such as PF_5 ,^{4a} PCl_5 ,^{4b} AsF_5 ,^{4c} SbCl_5 ,^{4d} VF_5 ,^{4e} NbF_5 ,^{4f} NbCl_5 ,^{4g} TaF_5 ,^{4f} TaCl_5 ,^{4g} and TaBr_5 ,^{4h} are of the second. On the other hand, the pentahalides of atoms from group 6 appear to have distorted trigonal-bipyramidal structures

(CrF_5^{5a}) or to be a mixture of trigonal-bipyramidal and tetragonal-pyramidal forms (MoCl_5^{5b} and WCl_5^{5c}).

There are some interesting questions about the structures of the group 8 five-coordinate molecules. A number of investigations have confirmed that $\text{Fe}(\text{CO})_5$ has D_{3h} symmetry both in the gas phase⁶⁻⁹ and in the crystal.¹⁰ There is controversy, however, about the relative lengths of the axial and equatorial Fe-C bonds: it has been concluded from the results of electron-diffraction studies⁹ that, in contrast to what is found for other D_{3h} pentacoordinate molecules, the axial bonds in $\text{Fe}(\text{CO})_5$ are the shorter. Work in this laboratory¹¹ revealed that the effects of vibrational averaging, which were not thoroughly investigated in the earlier diffraction work, play an especially important role in the determination of the relative bond lengths, and accordingly the relative bond lengths are still

(1) (a) Oregon State University. (b) Simon Fraser University.

(2) (a) Gillespie, R. J.; Nyholm, R. S. *Q. Rev., Chem. Soc.* **1957**, *11*, 339.

(b) Gillespie, R. J. *Molecular Geometry*; Van Nostrand-Reinhold: London, 1972.

(3) Heenan, R. K.; Robiette, A. G. *J. Mol. Struct.* **1979**, *55*, 191.

(4) (a) See, for example: Kurimura, H.; Yamamoto, S.; Egawa, T.; Kuchitsu, K. *J. Mol. Struct.* **1986**, *140*, 79 and references cited therein. (b) Adams, W. J.; Bartell, L. S. *J. Mol. Struct.* **1971**, *8*, 23. See also: McClelland, B. W.; Hedberg, L.; Hedberg, K. *J. Mol. Struct.* **1983**, *99*, 309. (c) Clippard, F. B.; Bartell, L. S. *Inorg. Chem.* **1970**, *9*, 805. (d) Ivashkevich, L. S.; Ischenko, A. A.; Spiridonov, V. P.; Strand, T. G.; Ivanov, A. A.; Nikolaev, A. N. *Zh. Strukt. Khim. (Engl. Transl.)* **1982**, *23*, 295. (e) Hagen, K.; Gilbert, M. M.; Hedberg, L.; Hedberg, K. *Inorg. Chem.* **1982**, *21*, 2690. (f) Petrova, V. N.; Girichev, G. V.; Petrov, V. M.; Goncharuk, V. K. *Zh. Strukt. Khim. (Engl. Transl.)* **1985**, *26*, 192. (g) Ischenko, A. A.; Strand, T. G.; Demidov, A. V.; Spiridonov, V. P. *J. Mol. Struct.* **1978**, *43*, 227. (h) Demidov, A. V.; Ivanov, A. A.; Ivashkevich, L. S.; Ischenko, A. A.; Spiridonov, V. P.; Almlöf, J.; Strand, T. G. *Chem. Phys. Lett.* **1979**, *64*, 528.

(5) (a) Jacob, E. J.; Hedberg, L.; Hedberg, K.; Davis, H.; Gard, G. L. *J. Phys. Chem.* **1984**, *88*, 1935. (b) Brunvoll, J.; Ischenko, A. A.; Spiridonov, V. P.; Strand, T. G. *Acta Chem. Scand., Ser. A*, in press. (c) Ezhov, Yu. S.; Sarvin, A. P. *Zh. Strukt. Khim. (Engl. Transl.)* **1983**, *24*, 140.

(6) Davis, M.; Hanson, H. P. *J. Phys. Chem.* **1965**, *69*, 3405. (7) Beagley, B.; Cruickshank, D. W. J.; Pinder, P. M.; Robiette, A. G.; Sheldrick, G. M. *Acta Crystallogr., Sect. B: Struct. Crystallogr. Cryst. Chem.* **1969**, *B25*, 737.

(8) Almenningen, A.; Haaland, A.; Wahl, K. *Acta Chem. Scand.* **1969**, *23*, 2245.

(9) Beagley, B.; Schmidling, D. G. *J. Mol. Struct.* **1974**, *22*, 466.

(10) (a) Hanson, A. W. *Acta Crystallogr.* **1962**, *15*, 930. (b) Donohue, J.; Caron, A. *Acta Crystallogr.* **1964**, *17*, 663.

(11) Unpublished work.